ARTICLE

Insight into Capture of Greenhouse Gas (CO$_2$) based on Guanidinium Ionic Liquids

He-xiu Liu[a,b], Rui-lin Man[a*], Bai-shu Zheng[b], Zhao-xu Wang[b], Ping-gui Yi[b]

a. School of Chemistry and Chemical Engineering, Central South University, Changsha 410083, China
b. Key Laboratory of Theoretical Chemistry and Molecular Simulation of Ministry of Education, Hunan University of Science and Technology, Xiangtan 411201, China

Quantum mechanics and molecular dynamics are used to simulate guanidinium ionic liquids. Results show that the stronger interaction exists between guanidine cation and chlorine anion with interaction energy about 109.216 kcal/mol. There are two types of spatial distribution for the title system: middle and top. Middle mode is a more stable conformation according to energy and geometric distribution. It is also verified by radial distribution function. The continuous increase of carbon dioxide (CO$_2$) does not affect the structure of ionic liquids, but CO$_2$ molecules are always captured by the cavity of ionic liquids.

Key words: Ionic liquids, Quantum chemical calculation, Molecular dynamics simulation, Interaction energy, Radial distribution

I. INTRODUCTION

Ionic liquid is a new type of liquid compound with low melting point, low vapor pressure, high solubility, and high heat stability [1−4]. Green ionic liquid is the ionic liquid made up of recycled cations and anions, which has less volatile, recycled characteristics and is in line with the green chemistry. Over the past twenty years, synthesis of green medium and functional materials has received extensive attention from the domestic and international academic and industrial fields. The "programmable" feature of ionic liquids makes it possible to adjust its physical and chemical properties by changing the type and size of cations or anions and to design the ionic liquid with special function according to specific applications and needs. Great progress has been made in the application and research of ionic liquids so far, which has been widely used as a solvent, reaction medium, catalyst and functional material in the synthesis and catalysis, extraction and separation, electrochemistry, biological chemistry and other fields [5].

In recent years, the climate warming caused by CO$_2$ has become one of the focuses on environmental issues in the world. It is urgent to solve the problem of CO$_2$ greenhouse effect. But the CO$_2$ is a safe and abundant carbon resource from a point of recycling. The gaseous CO$_2$ can be used as a fertilizer and sterilization, *etc.* Supercritical CO$_2$ can also be used for food, pharma-

ceutical and other industries. Solid CO$_2$ can be used for artificial rainfall, concrete production and environmental protection, *etc.* Therefore, there is important scientific significance in fixing and recovering CO$_2$ industrially. Existing CO$_2$ fixation technologies such as biological method, physical method and chemical method have some limitations that carbon resource waste and organic solvent volatilization can lead to the problems of environment pollution, the equipment corrosion and post-processing complexity. Because of the features of low vapor pressure and strong dissolving ability of the ionic liquid, to fix CO$_2$ using ionic liquids has attracted great attentions. There are the following advantages in applying ionic liquid to fix CO$_2$. The CO$_2$ recycling use takes the place of the direct abandon of traditional method. Nature of the ionic liquid is stable, non-volatile and recycled. It is shown that ionic liquids have good abilities to absorb and dissolve CO$_2$ and show effective catalytic or sub-catalytic performances in the CO$_2$ conversion reaction under certain conditions [6−10].

Compared with imidazoles and phosphonium salt, guanidinium ionic liquid has more significant thermal and chemical stability, better catalytic activity and stronger biological activity *etc.* [11−13]. In addition, the charge dispersion degree is high in guanidine salt cation. Moreover, the different substituent on the three nitrogen atoms and the counter anions can be directionally designed and chosen in order to make the ionic liquid own some excellent physical or chemical properties. For example, Wang *et al.* studied the force field of the TMGL ionic liquid and the solubility of SO$_2$ and CO$_2$ from molecular danymics simulation [14]. Zhang *et al.* investigated the microscopic structure, interactions, and properties of pure ionic liquid [ppg][BF$_4$]

---

*Author to whom correspondence should be addressed. E-mail: rlman@mail.csu.edu.cn, hxliu12@hnust.edu.cn

and mixtures of [ppg][BF$_4$] and CO$_2$ by molecular dynamics (MD) simulations and *ab initio* calculations [15]. Zhang *et al.* reported the solubilities of CO$_2$ in 1-butyl-3-methylimidazolium hexafluorophosphate and 1,1,3,3-tetramethylguanidium lactate at elevated pressures [16]. Therefore, it is important to investigate the interaction between guanidinium ionic liquids and CO$_2$ gas molecules, study the influence of the structure of ionic liquid on the absorption of such gas, and understand further the mechanism that guanidinium ionic liquids absorb CO$_2$ gas by quantum chemistry calculation and MD simulation from molecular level, which can provide theoretical basis for designing and developing new high absorptive guanidinium ionic liquids. To the best of our knowledge, there are no reported calculations involving the guanidine cation, chlorine anion and CO$_2$ systems. In the present work, we report results of the quantum mechanics and molecular dynamics on the guanidine cation and the chlorine anion systems, and guanidine cation and the chlorine anion-CO$_2$ systems and seek to develop an understanding of the capture ability of the guanidine cation and the chlorine anion ionic liquid toward the CO$_2$ gas.

II. FUNDAMENTAL THEORIES AND COMPUTATIONS DETAILS

The initial structure may be top, side and middle type (Fig.1) for the simple guanidinium interacting with anion because there are a variety of modes of interaction for guanidinium ion pair. The second order perturbation theory (MP2) and density functional method (X3LYP) with 6-311++G (d,p) and aug-cc-PVDZ basis set are adopted to optimize monomers and dimers for possible initial configuration. Two stable configurations are got: top and middle type. The main anionic attack method can be initially determined as middle type through the analysis of electrostatic potential of monomer and the highest occupied orbital. The binding energy of the compound can be calculated according to the equation:

$$\Delta E_{\text{int}} = E_{\text{dimer}} - (E_{\text{mono,1}} + E_{\text{mono,2}}) + \text{BSSE} \quad (1)$$

here $E_{\text{mono,1}}$, $E_{\text{mono,2}}$, and E_{dimer} represent the energy of cation, anion, and the dimer respectively. The basis set superposition error (BSSE) approach was incorporated into the calculations via the counterpoise (CP) method proposed by Boys and Bernardi [17]. All calculations in this work were performed using the Gaussian 03 package [18].

In molecular dynamics simulation, we adopted Gromacs 4.5.4 package [19, 20], combined with OPLS-AA/L atomic force field developed by Lopes and others [21]. The parameters of cationic and anionic force field come from the program. The force field parameters of CO$_2$ are from Ref.[22]. 128 cations and 128 anions are added in the initial structures randomly, followed that
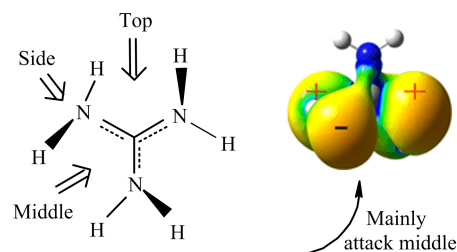

FIG. 1 The anions attacking on three positions of the guanidinium cation and the HOMO(16) mapped with electronic potential from total SCF density of guanidinium.
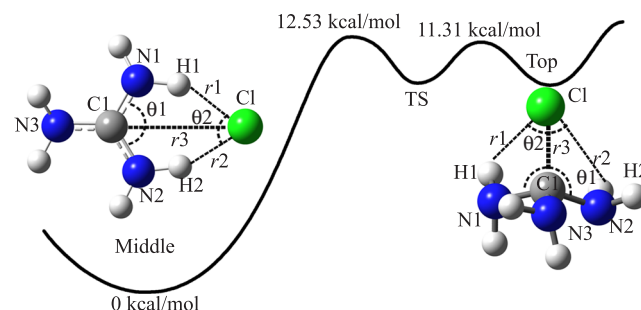

FIG. 2 Methanetriamine positive ion (METM$^+$) and Cl$^-$ in different geometries (middle, top).

0, 8, 18, 36, and 64 CO$_2$ molecules are joined respectively. The energy minimization of 500 ps and the steepest descent method are used in the simulation. When the maximum force converges in 100 kJ·mol·nm, the NPT system simulation is adopted. Berendsen algorithm is applied in the temperature control and pressure control [23]. The Newtonian motion equations are solved by leapfrog (leap-frog) algorithm in which time step is set to 2 fs. The linear constraint solver [24] are used in the restrictive algorithm of bond in which the truncation radius is 1.4 nm [25]. The particle mesh Ewad algorithm is applied in long-range electrostatic interaction [26, 27]. The temperature and pressure are 460 K and 1.0 bar respectively. When NPT reaches the convergence criteria, the 5 ns MD simulation is carried out finally. The temperature and pressure are controlled by the Nose-Hoover algorithm [28] and Parrinello-Rahman algorithm [29].

III. RESULTS AND DISCUSSION

The geometric configurations of intermolecular interactions between guanidinium cation and chlorine anion are optimized by MP2 with 6-311++G(d,p) basis set and X3LYP with 6-311++G(d,p) and aug-cc-pvdz basis set. The structures of these compounds are shown in Fig.2. The related geometry parameters and the binding energies are listed in Table I. The optimization results show that there are two different types for the intermolecular interaction between guanidine

TABLE I Dimer geometry and interaction energy (E_{int}) of guanidine ionic liquid.

	Methods	R(N1−C1)/Å	R(N2−C1)/Å	$\theta1/(°)$	$\theta2/(°)$	$r1$/Å	$r2$/Å	$r3$/Å	E_{int}/(kcal/mol)
METM$^+$	MP2/6-311++G**	1.334	1.334	120.0					
	X3LYP/6-311++G**	1.334	1.334	120.0					
	X3LYP/aug-cc-pvdz	1.337	1.337	120.0					
Middle	MP2/6-311++G**	1.330	1.324	119.0	63.4	1.986	1.940	3.393	−107.521
	X3LYP/6-311++G**	1.328	1.324	118.9	62.9	2.018	2.037	3.452	−109.216
	X3LYP/aug-cc-pvdz	1.328	1.328	118.8	63.6	2.017	2.017	3.443	−113.413
Top	MP2/6-311++G**	1.418	1.424	108.2	54.4	2.674	2.971	1.928	−91.512
	X3LYP/6-311++G**	1.440	1.418	114.3	54.4	2.674	2.971	1.928	−85.907
	X3LYP/aug-cc-pvdz	1.447	1.419	114.4	54.6	2.665	2.963	1.932	−86.751

salt cation and chlorine anion which are middle and top. Figure 2 shows hydrogen bonds are formed between chlorine anion and two side hydrogen of guanidinium cation in the middle configuration, while C−Cl bond is formed between C$^+$ ion of guanidine salt cation and chlorine anion for the top configuration. According to the structure parameters of compounds and the monomers in Table I, the bond lengths of the complexes all have certain changes compared with monomers. The bond lengths of R(N1−C1) and R(N2−C1) decrease in middle configurations, while increase in the top configuration compounds. All these bond length changes are caused by the weak interaction between the two monomers.

According to results listed in Table I, the distances of two hydrogen bond in the middle configuration are 2.018 ($r1$), 2.037 Å ($r2$) at the X3LYP/6-311++G(d,p) computational level respectively, which indicates that the hydrogen bond formed between the guanidinium cation and chlorine anion is stronger. The distances ($r1$, $r2$) of hydrogen bonds in top configuration compound are slightly larger than the corresponding data in middle complex, which are 2.674 and 2.971 Å respectively. Obviously, the middle mode is more stable than the top one for the intermolecular interactions between the guanidinium cation and chlorine anion. For middle configuration compounds, this function mode is more advantageous over the molecular space distribution. For the molecular point group of METM$^+$ is C2, it can still keep the characteristics of C2 point group after it interacts with chloride ion. When more ion pairs interact, single cation can accommodate three Cl$^-$ ions and six hydrogen atoms can all form hydrogen bonds in space. Top model is not conducive to the accumulation of many molecules because its symmetry falls. The guanidinium cation can only hold 1 or 2 Cl$^-$ ions. From the perspective of the spatial distribution characteristics of ion pairs in the interaction between guanidinium cationic ions and chlorine anionic ions, the model of the middle is more advantageous over the pattern of the top. In addition, energy variation characteristics of two kinds of patterns are analyzed in this work. It needs 12.5 kcal/mol energy barriers in the process of the mid-
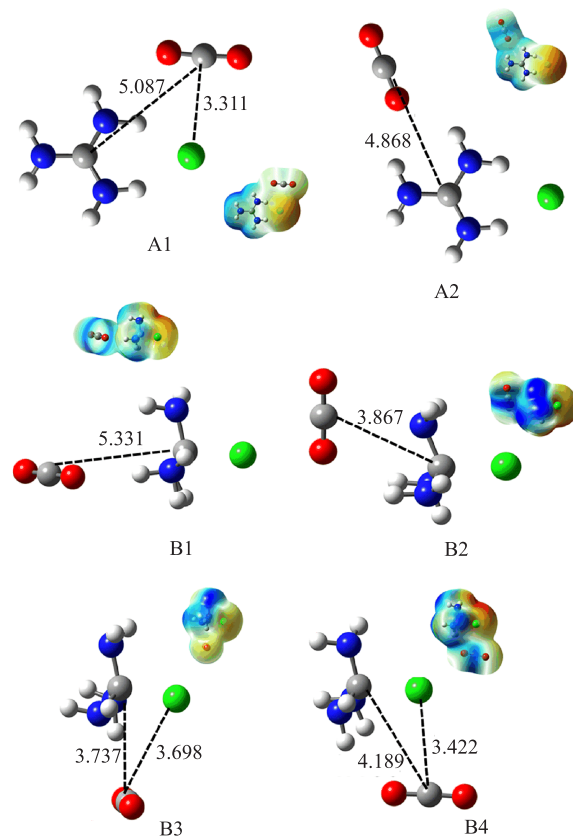
FIG. 3 Conformations of the guanidinium cation and the chlorine anion by capturing CO_2 molecule.

dle configuration changing into the top structure, which makes the middle mode in the ionic liquid more stable than the top one. At the same time, we can also see middle configuration has larger interaction energy under different methods and basis set from Table I, which explains that the intermolecular interaction is stronger. In short, middle interaction mode is the main spatial distribution pattern in title system.

In order to further investigate the capacity of guanidinium ionic capturing CO_2, density functional method X3LYP/6-311++G(d,p) and molecular dynamics simu-
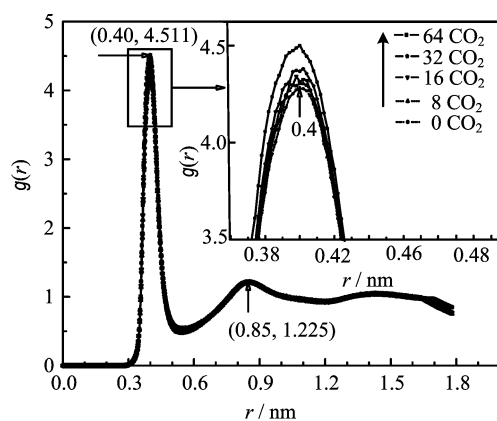
FIG. 4 Radial distribution functions graph between the carbocation and chlorine anion in the different number of CO_2.

FIG. 5 The cumulative particle number of Cl^- changing with the distance.

lations are used to investigate the microstructure characteristics of weak interactions between guanidinium ionic pairs and CO_2 molecules. The computational results are shown in Fig.3 and Fig.4. Obviously, it is not difficult to find from the Fig.3 that CO_2 can not only form intermolecular interaction with $METM^+$, but also form intermolecular interaction with the ionic pairs of cation and anion according to the spatial distribution characteristics from A1 to B4. But there isn't intermolecular interaction between CO_2 and anion. For example, it can be seen from the electrostatic potential chart of the B2 configuration that the negatively charged center of CO_2 located at the two oxygen atoms, while the electrostatic potential of Cl^- is a red area which indicates that the potential is negative. It is consistent with electrostatic distribution of the two oxygen atoms of CO_2 which hinders the interaction between CO_2 and Cl^-. Similarly, the same conclusions can also be drawn for other configuration analysis. It is worth mentioning that the introduction of CO_2 gas molecules has no larger influence on middle and top configurations of cationic and anionic pairs from the structure of interaction between guanidinium ion pair and CO_2 gas molecules.

In order to better illustrate the space characteristics of intermolecular interaction between guanidinium ionic pair and CO_2 gas molecular, the radial distribution functions of the mixed system are analyzed by the molecular dynamics simulation in this work. The influences of CO_2 on the microscopic structures and dynamics properties of guanidinium ionic liquids is also investigated. Radial distribution function $g(r)$ is the physical quantities of reaction fluid microstructure characteristics [30, 31]. As can be seen from the distribution characteristics, Cl^- mainly distributes in the largest peak (0.40, 4.511) (see Fig.4). The cumulative particle number of Cl^- changes with the distance, as shown in Fig.5. About 2.02 Cl^- ions appear around the location (r=0.4) which is consistent with the cationic space filled with three Cl^- ions. With the increase of the distance of
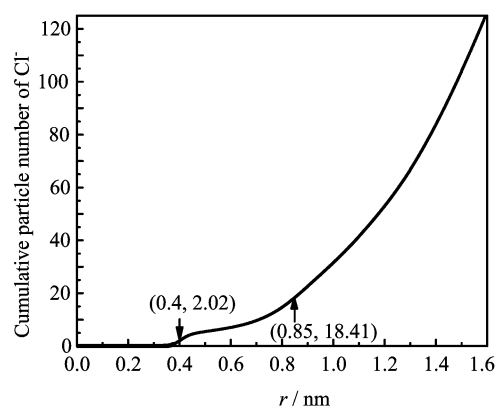
cation and anion, Cl^- ion number is increased to about 18.41 when the distance arrives at 0.85 nm. The curve flattens out with the distance from 1.0 nm to 2.0 nm which explains that the emergence probability of anion has a logarithmic growth trend. The maximum location (0.40, 4.511) of radial distribution function is very close to 3.39 Å, which can also be concluded that middle model in the research system is the main way of spatial distribution. It is worth noting that the 0.4 nm is larger about 0.6 Å than 3.39 Å, which is caused by more than one counter charge ion in a large number of ionic liquids, leading to the weakened interaction between cation and anion. Currently, Bern group and Cadena team found that the cavities are closely associated with the capture process of CO_2. Moreover, Bern *et al.* also drew the conclusion that the addition of CO_2 molecules didn't influence the imidazoles structure of ionic liquids obviously when they simulated the system of imidazoles ionic liquids and CO_2. They think there are some cavities in the ionic liquid, which enable the CO_2 molecules not to destroy the microscopic structure of the ionic liquid when they enter into the cavities [32, 33]. It can be seen from Fig.4 that there is no apparent difference in radial distribution function in the ionic liquid system with 8, 16, 32, and 64 CO_2 molecules which further indicates that the addition of CO_2 molecules has no big impact on the microstructure between cation and anion in the guanidinium ionic liquid system.

According to the above results of quantum chemical calculation and molecular dynamics simulation, it can be seen that the interaction distance of $METM^+$ and Cl^- is 0.40 nm when the cation and the anion are in the condition of 8, 16, 32, and 64 CO_2 molecule which is almost consistent with the distance of 0.4 nm when there are no CO_2 molecules. It further illustrates that there may be some cavities in guanidinium ionic liquid which is similar to imidazoles ionic liquids. These cavities of guanidiniun ionic pairs play a major maintenance role in the process of capturing CO_2 molecules.

IV. CONCLUSION

The structure characteristics of guanidinium ionic liquids and the mechanism of guanidinium ionic liquids capturing CO_2 molecular are investigated by quantum chemical calculation and molecular dynamics simulation theoretically. There is stronger interaction between guanidine cation and chlorine anion. Their interaction model is given priority to middle mode. The dissolution of CO_2 gas molecules in the guanidinium ionic liquid hasn't obvious influence on the structure of the ionic pair. The conclusions state that the guanidinium ionic liquid is similar to the imidazole ionic liquid. It may have some cavities in which CO_2 gas molecules mainly exist. This project can provide theoretical basis for designing and developing new high absorptive guanidinium ionic liquids.

V. ACKNOWLEDGMENTS

[1] Y. Wang, H. Li, and S. Han, J. Phys. Chem. B **110**, 24646 (2006).

[2] M. Yizhak, J. Chem. Thermodyn. **48**, 70 (2012).

[3] Y. Xu, J. Yao, C. Wang, and H. Li, J. Chem. Eng. Data **57**, 298 (2012).

[4] A. Suvitha and P. Murugakoothan, Spectrochim. Acta Part A **86**, 266 (2012).

[5] H. Sun, *Theoretical Studies on Structure and Catalytic Mechanism of Several Ionic Liquid*, Ji'nan: Shandong University, (2010).

[6] H. B. Chen and J. Yu, Chem. Thchno-Econo. **21**, 11 (2003).

[7] Y. L. Pang, Chem. Ind. Eng. Process **27**, 1363 (2008).

[8] S. M. Yao, X. G. Wang, H. Zhang, and Z. Y. Liu, Chem. Ind. Eng. Process **27**, 640 (2008).

[9] C. M. Wang, G. K. Cui, X. Y. Luo, Y. J. Xu, H. R. Li, and S. Dai, J. Am. Chem. Soc. **133**, 11916 (2011).

[10] A. F. Ghobadi, V. Taghikhani, and J. R. Elliott, J. Phys. Chem. B **115**, 13599 (2011).

[11] S. Li, Z. L. Li, Y. L. Hu, X. F. Gao, and X. R. Huang, Chem. J. Chin. Univ. **6**, 1339 (2011).

[12] H. L. Rust, C. I. Zurita-Lopez, S. Clarke, and P. R. Thompsom, Biochemistry **50**, 3332 (2011).

[13] A. K. Choudhury, S. Y. Golovine, and L. M. Dedkova, S. M. Hecht, Biochemistry **46**, 4066 (2007).

[14] Y. Wang, H. H. Pan, H. R. Li, and C. M. Wang, J. Phys. Chem. B **111**, 10461 (2007).

[15] X. C. Zhang, X. M. Liu, X. Q. Yao, and S. J. Zhang, Ind. Eng. Chem. Res. **50**, 8323 (2011).

[16] S. J. Zhang, X. L.Yuan, Y. H. Chen, and X. P. Zhang, J. Chem. Eng. Data **50**, 1582 (2005).

[17] S. F. Boys and F. Bernardi, Mol. Phys. **19**, 553 (1970).

[18] M. J. Frisch, G. W. Trucks, H. B. Schlegel, G. E. Scuseria, M. A. Robb, J. R. Cheeseman, J. A. Jr. Montgomery, T. Vreven, K. N. Kudin, J. C. Burant, J. M. Millan, S. S. Iyengar, J. Tomasi, V. Barone, B. Mennucci, M. Cossi, G. Scalmani, N. Rega, G. A. Petersson, H. Nakatsuji, M. Hada, M. Ehara, K. Toyota, R. Fukuda, J. Hasegawa, M. Ishida, T. Nakajima, Y. Honda, O. Kitao, H. Nakai, M. Klene, X. Li, J. E. Knox, H. P. Hratchian, J. B. Cross, C. Adamo, J. Jaramillo, R. Gomperts, R. E. Stratmann, O. Yazyev, A. J. Austin, R. Cammi, C. Pomelli, J. W. Ochterski, P. Y. Ayala, K. Morokuma, G. A. Voth, P. Salvador, J. J. Dannenberg, V. G. Zakrzewski, S. Dapprich, A. D. Daniels, M. C. Strain, Ö. Farkas, D. K. Malick, A. D. Rabuck, K. Raghavachari, J. B. Foresman, J. V. Ortiz, Q. Cui, A. G. Baboul, S. Clifford, J. Cioslowski, B. B. Stefanov, G. Liu, A. Liashenko. P. Piskorz, I. Komaromi, R. L. Martin, D. J. Fox, T. Keith, M. A. Al-Laham, C. Y. Peng, A. Nanayakkara, M. Challacombe, P. M. W. Gill, B. Johnson, W. Chen, M. W. Wong, C. Gonzalez, and J. A. Pople, *Gaussian 03, Revision D.03.* Pittsburgh, PA: Gaussian, Inc., (2003).

[19] H. J. C. Berendsen, D. van der Spoel, and R. van Drunen, Comput. Phys. Commun. **91**, 43 (1995).

[20] E. Lindahl, B. Hess, and D. Van Der Spoel, J. Mol. Model. **7**, 306 (2001).

[21] J. N. Canongia Lopes, J. Deschamps, and A. A. H. Pádua, J. Phys. Chem. B **108**, 11250 (2004).

[22] W. Shi and E. J. Maginn, J. Phys. Chem. B **112**, 2045 (2008).

[23] H. J. C. Berendsen, J. P. M. Postma, W. F. van Gunsteren, A. DiNola, and J. R. Haak, J. Chem. Phys. **81**, 3684 (1984).

[24] B. Hess, H. Bekker, H. J. C. Berendsen, and J. G. E. M. Fraaije, J. Comput. Chem. **18**, 1463 (1997).

[25] M. Levitt, M. Hirshberg, R. Sharon, and V. Daggett, Comput. Phys. Commun. **91**, 215 (1995).

[26] U. Essmann, L. Perera, M. L. Berkowitz, T. Darden, H. Lee, and L. G. Pedersen, J. Chem. Phys. **103**, 8577 (1995).

[27] T. Darden, D. York, and L. Pedersen, J. Chem. Phys. **98**, 10089 (1993).

[28] W. G. Hoover, Phys. Rev. A **31**, 1695 (1985).

[29] M. Parrinello and A. Rahman, J. Appl. Phys. **52**, 7182 (1981).

[30] M. Winter, *Webelements Periodic Table*, Sheffield: The University of Sheffield and WebElements Ltd. (2004).

[31] E. Lindahl and O. Edholm, J. Chem. Phys. **115**, 4938 (2001).

[32] X. Huang, C. J. Margulis, Y. Li, and B. J. Berne, J. Am. Chem. Soc. **127**, 17842 (2005).

[33] C. Cadena, J. L. Anthony, J. K. Shah, T. I. Morrow, J. F. Brennecke, and E. J. Maginn, J. Am. Chem. Soc. **126**, 5300 (2004).